Electrets substituting external bias voltage in dielectric elastomer generators: application to human motion

Smart Mater. Struct. **22** (2013) 025012 (13pp) doi:10.1088/0964-1726/22/2/025012

Electrets substituting external bias voltage in dielectric elastomer generators: application to human motion

T Vu-Cong[1], C Jean-Mistral[2] and A Sylvestre[1]

[1] Grenoble Electrical Engineering Laboratory (G2ELab), Joseph Fourier University (UJF), G-INP, CNRS, 25 rue des Martyrs, BP166, F-38402 Grenoble, Cedex 9, France
[2] Mechanics Laboratory of Contacts and Structures (LaMCoS), University of Lyon, INSA, CNRS , 18-20 rue des sciences, F-69621 Villeurbanne Cedex, France

E-mail: cong-thanh.vu@g2elab.grenoble-inp.fr

Received 5 August 2012, in final form 30 October 2012
Published 9 January 2013
Online at stacks.iop.org/SMS/22/025012

Abstract
Dielectric elastomer generators offer great potential for soft applications involving fluid or human interactions. These scavengers are light, compliant, have a wide range of functions and develop an important energy density. Nevertheless, these systems are passive and require an external bias source, namely a high voltage source and complex power circuits. This cumbersome polarization complexes the system in a drastic way and slows down the development of dielectric generators. In order to remove these problems, we propose here new transducers based on the use of an electret coupled with dielectric elastomer, thus avoiding the use of a high external voltage source, and leading to the design of a soft autonomous dielectric generator. By combining a dielectric model and the electret theory, an electromechanical model was developed to evaluate the capabilities of such a generator. This generator was then produced starting from Teflon^{TM} as electret and silicone PolyPower^{TM} as electroactive polymer. A good agreement between the model and the experiment were obtained. An experimental energy density of 0.55 mJ g^{-1} was reached for 50% strain (electret potential of −1000 V). Once optimized in its design, such a soft generator could produce energy density up to 1.42 mJ g^{-1}. An energy density of 4.16 mJ g^{-1} is expected with an electret potential of −2000 V.

(Some figures may appear in colour only in the online journal)

1. Introduction

The challenge of battery-free devices is moving towards turning into reality, thanks to the development of energy scavengers. Electromagnetic or piezoelectric devices have already replaced batteries as in flashlights, and widespread photovoltaic applications (phone chargers…) [1, 2]. For soft applications involving human interaction or fluid interaction (water, wind), dielectric elastomer generators (DEGs) have a great potential for development. These scavengers are lightweight, low cost, compliant and can adopt complex shapes. They can convert linear or rotational motions with few mechanical transmission mechanisms (gears, belts, …), and work on a broad range of frequencies and also of amplitudes. Dielectric elastomers have good performance in terms of energy density in both theoretical analysis and experimental investigations. The theory of elastic dielectrics predicted a high energy density recoverable with the VHB elastomer, of about 1.7 J g^{-1}, by studying the region of allowable states for operation, which is limited by various modes of failure such as electromechanical instability, electrical breakdown, mechanical rupture and loss of tension [3]. While focusing on experiments, one can highlight that, in 2008, Chiba *et al* proposed the first ocean-wave generator made of dielectric elastomer in a roll configuration (150 g) and producing up to 12 J for one cycle (energy density of 0.08 J g^{-1}), but

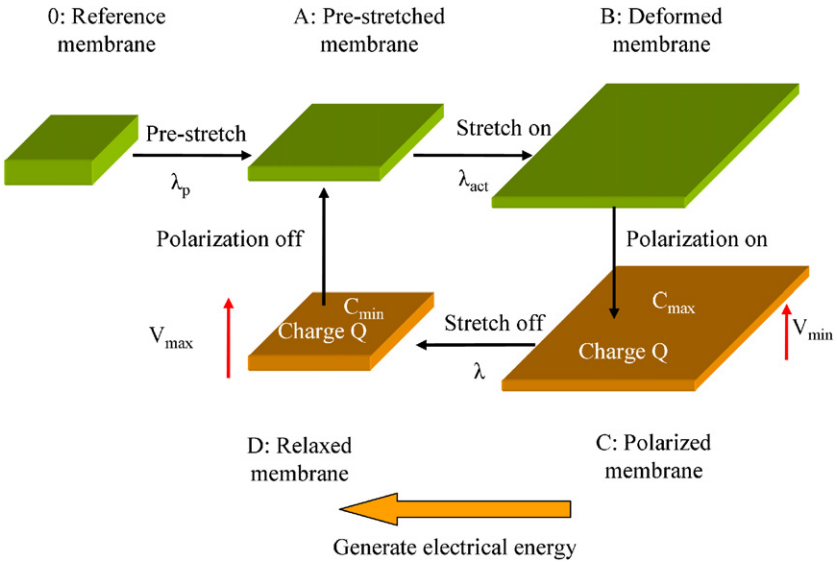

Figure 1. Energetic cycle for dielectric elastomer generator.

with a bias voltage of 2 kV [4]. The second generation uses 220 g of active material for output energy of 25 J (energy density of 0.1 J g^{-1}). The energy harvesting circuit is quite simple and insures an efficiency of 78% [5]. More recently, Iskandarani *et al* have scavenged 94.5 mJ with the polymer PolyPower^{TM} from Danfoss, by conditioning the material under 15% of strain and 1.8 kV of poling voltage during a cycle at constant charge Q [6]. The generator proposed by McKay *et al*, also using a high bias voltage (2 kV), is able to scavenge an average output power up to 0.8 mW [7]. From another approach, Jean-Mistral *et al* have chosen to develop dielectric elastomer generators working under moderate voltages. Thus, they created a patch that harvests energy from a human knee movement while walking [8]. This structure is designed to produce 100 μW with a bias voltage of 170 V, but can easily produce up to 1.74 mW under a poling voltage of 1 kV. Despite the high scavenged energy density, all these scavengers require a high external bias voltage. This polarization source is classically a high voltage supply [4, 8], a pump charge circuit [7] or a more complex power circuit such as bidirectional flyback [9]. In addition, these power circuits use transformers and a lot of switches, which make them heavy and complex, and can introduce significant delays before starting the scavenging process.

In spite of the complex power circuit, dielectric elastomer generators are still a promising candidate to scavenge energy from human motion, but not a reality. Indeed, these circuits are not yet integrated and can interfere with normal human walking. Our solution to this issue is to replace the external bias voltage by an electret in order to design a completely autonomous and lightweight dielectric elastomer generator. Our contribution is to demonstrate the ability of combining these two materials electrically and mechanically.

In the remainder of this paper, section 2 introduces the design of the imagined soft generator associating an electret (to replace the high voltage supply) and the dielectric elastomer. In section 3, we develop an accurate analytical model for this new concept of generator, its implementation (Matlab/Simulink) and its validation using a finite element method (FEM). From this model, the structure can be designed with better performance. Lastly, in section 4, the capabilities of the manufactured soft electrostatic generator are tested and compared with the results of the model. For a given mechanical strain of 50%, an energy density of approximately 0.55 mJ g^{-1} was produced.

2. Principle of conversion

Basically, a dielectric elastomer generator is made of an elastically deformable insulating polymer which is coated on each side with a compliant electrode. A dielectric elastomer generator is an electrostatic generator converting the mechanical work, related to the deformation of the polymers, into electrical energy because of capacitance variations. Figure 1 shows the classic energetic cycle and (1) translates the associated produced energy for a cycle at constant charge Q.

$$E_{pro} = \tfrac{1}{2}(C_{min}V_{max}^2 - C_{max}V_{min}^2). \quad (1)$$

C_{min} and C_{max} are the minimal and maximal capacitances respectively in states D and C of the cycle depicted in figure 1. V_{max} and V_{min} are the maximal and minimal voltages in the same states.

The charge (phase B–C in figure 1) and discharge (phase D–A) processes are applied during the two limit states: maximum and minimum capacitance. The conversion mechanism takes place when such structures switch from the high to the low value of capacitance (phase C–D).

All classical cycles (constant charge Q, constant voltage V and constant electric field E) need initial polarization energy: a step-up voltage converter has to be a part of the generator circuit as shown in figure 2(a).

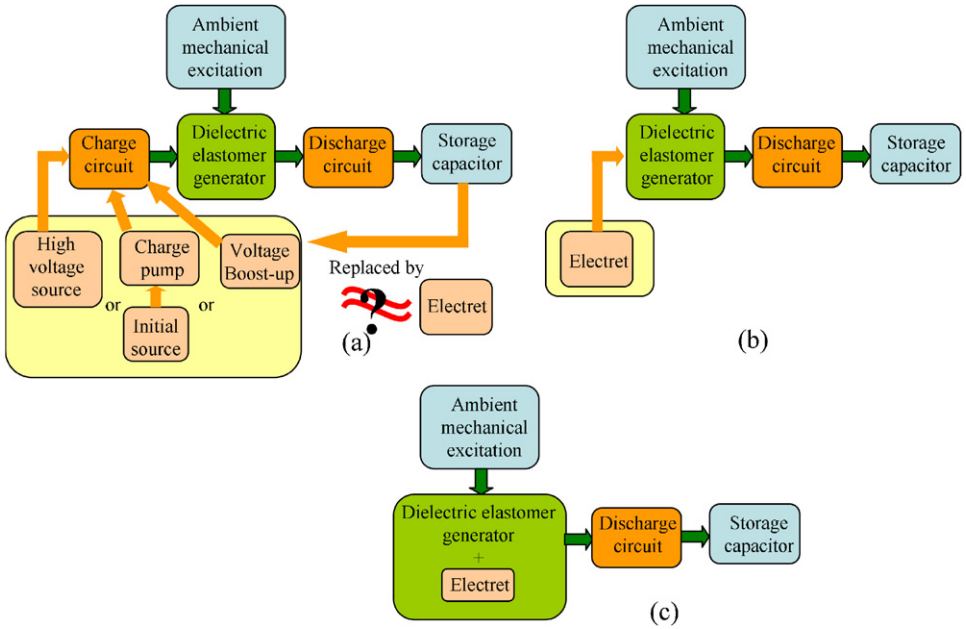

Figure 2. Schematic dielectric elastomer generator. (a) Conventional dielectric elastomer generator. (b) Dielectric elastomer generator with electret as a polarization source. (c) Electret–dielectric elastomer generator.

The step-up voltage is the major disadvantage of dielectric elastomer generators, which limits the development and implantation of such transducers in wearable applications. Thus, we proposed to associate a dielectric elastomer and an electret (i.e. quasi-permanent charged dielectric) to build an autonomous soft generator. The electret can be used as an electrostatic source to polarize the dielectric elastomer replacing the charge circuit (figure 2(b)), or the dielectric can be introduced into an electret generator to increase its performance (figure 2(c)).

In figure 2(b) (first mode), the electret with its intrinsic electric field must induce a static electric field into the dielectric elastomer to polarize it. Keplinger *et al* have studied the deformation of dielectric elastomer placed nearby the needle of a corona discharge equipment [10]. The electrical field generated by needles led to an electrical field in the elastomer, thus deforming the material. Based on the same idea, without electrical connection between electrets and elastomer, electrets may for example be closer to or further away from a dielectric elastomer, leading to the creation or extinction of an electric field in the dielectric elastomer. This behavior allows the accomplishment of a polarization phase (phase B–C in figure 1) and thus a classic energetic cycle can be achieved. The power management can be simple with one diode [11].

In figure 2(c) (second mode), the scavenger has the same operating principle as a classic electret generator: re-arrangement of charges between two electrodes through a load by the changing capacitance. Indeed, let us compare dielectric elastomer generators with classic electrostatic generators. Electrostatic generators are typically resonant structures which harvest energy from vibrations thanks to capacitance variations. They also require a polarization and realize cycles as dielectric elastomer generator [12]. To avoid the use of an external supply voltage, one solution was to develop a transducer already polarized from electrets [13]. The first working electret generator appeared in 1978 and up to now they are generally used for MEMS applications and produce a low level of power under a moderate level of voltage (100 V) [14–16]. For example, Naruse *et al* produced 40 μW with their structure (9 cm^2) at 2 Hz [14]. Shimizu *et al* scavenged 10 μW at 20 Hz with a structure sizing of 4 cm^2 [15], and Edamoto *et al* developed a structure with low resonant frequency, allowed to scavenge 12 μW at 21 Hz, with an active surface of 3 cm^2 [16]. This second mode can be easily adapted to flexible structures thanks to organic electrets. As electrostatic generators go towards electret generators, dielectric elastomer generators change naturally into electret–dielectric elastomer generators.

Thus, we choose to develop in this paper an electret–dielectric elastomer generator. In order to simplify the associated power circuit, a maximal output voltage of 400 V is chosen. Low cost and low size classic electronic components can so be used for our scavenger prototype. Figure 3 introduces our new scavenger working as a soft electret generator. Electrets are solid dielectric materials with quasi-permanent electric potential: they can exhibit a high stable surface potential. Thanks to the trapping of charges, the electret develops a constant charge Q_i. Because of electrostatic induction and conservation of the charge, the sum of charges on the two electrodes is equal to the charges of the electret: $Q_i = Q_1 + Q_2$. When the device undergoes mechanical strain, the capacitance changes, which induces a reorganization of charges between electrodes through the load: an alternative current is generated across the electrical load R [14, 15]. Thus, a part of the mechanical energy is converted into electricity.

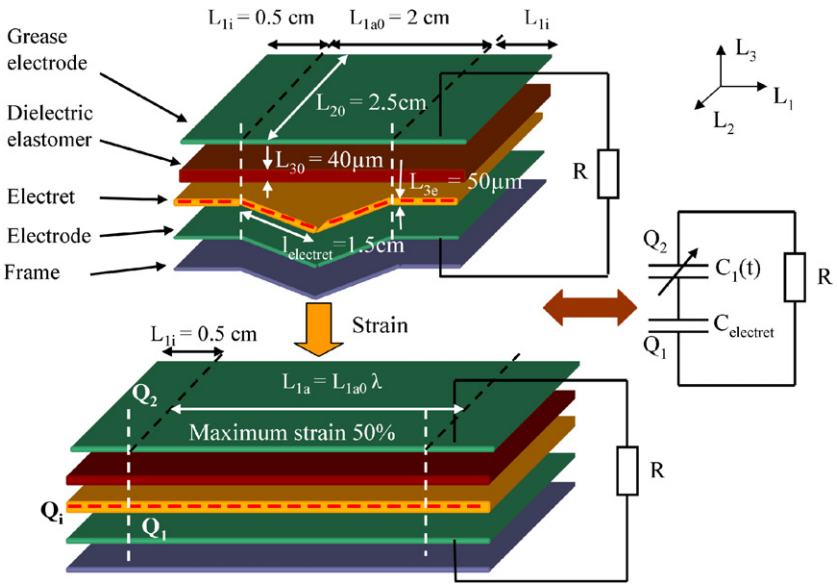

Figure 3. Design of electret–dielectric elastomer generator prototype: at-rest and maximal state.

Because of the electret is a rigid material, it cannot suffer large deformations as the dielectric elastomer can. Consequently, in order to be able to work under cycles in stretching, the generator is textured to circumvent this problem: realization of a 3D serpentine structure (figure 3). However, any reliable information on the behavior of the electret under stress is available in the literature: maybe the charges are dissipated and the surface potential decreases when the stress increases? To avoid this possible concern, the electret is unstrained and only the dielectric elastomer suffers huge deformations. The final structure is made up of a frame (rigid plastic), a rigid electrode (conductive tape—3M XYZ 9712), a non-deformable electret (Teflon FEP—DuPont), a dielectric elastomer (Danfoss PolyPower) and a conductive compliant electrode (carbon grease—MG Chemical). Conductive adhesive tape is used to glue the electret to the serpentine form of the frame. In the at-rest state, the air gap between the electret and the dielectric elastomer is the most distant compared to the state of working of the structure, thus inducing a small value of equivalent capacitance of this structure. When strain following the L_1 direction is imposed, only the active part (defined by L_{1a}) of the structure can be deformed; the inactive parts (described by L_{1i}) can only move between two pre-defined extreme positions (the at-rest and maximum strain states, as shown in figure 3). At the same time as the active part becomes deformed as a function of strain, the electret and the dielectric elastomer reduce their air gap, thus leading to an increase in the equivalent capacitance. At the maximum strain state, because of the absence of air gap between the two materials, the equivalent capacitance reaches its maximum value. One can note that the equivalent capacitance of our device varies as a function of imposed strain, which insures the mechanical–electrical conversion.

3. Analytic model of the soft generator

3.1. Theory

To determine the output power of the scavenger for a given mechanical solicitation, the equation of motion must be solved and the quantity of charge transferred to the electrical load must be determined. The mechanical equation of the structure can be written as

$$m\frac{\partial^2 \vec{L}_1}{\partial t^2} = \vec{F}_{\text{ext}} + \vec{F}_{\text{elas}} + \vec{F}_{\text{elec}}. \tag{2}$$

F_{ext} stands for the external mechanical force applied to the structure, F_{elas} is the elastic force developed by the dielectric elastomer and F_{elec} is the electrical force due to the electret. m is the mass and L_1 is the total length of our structure.

We suppose that the surface potential of the electret does not decrease with time: ideal electret. Thus, the equivalent electrical model of the device is presented in figure 4, where Q_1 and Q_2 are the charges in the lower and upper electrode respectively, V is the potential of the electret, R is the electrical load and C_{eq} is the equivalent capacitance of the structure. This equivalent capacitance consists of the electret's capacitance C_{electret}, the capacitance of the air gap C_{air} and the dielectric elastomer's capacitance $C_{\text{dielectric}}$ as expressed by (3).

$$\frac{1}{C_{\text{eq}}} = \frac{1}{C_{\text{dielectric}}} + \frac{1}{C_{\text{air}}} + \frac{1}{C_{\text{electret}}}. \tag{3}$$

Based on Kirchhoff's law, the current i and the differential equation governing the electrostatic system can be written as [17]

$$i(t) = \frac{\partial Q_2}{\partial t} = \frac{V}{R} - \frac{Q_2}{R}C_{\text{eq}}. \tag{4}$$

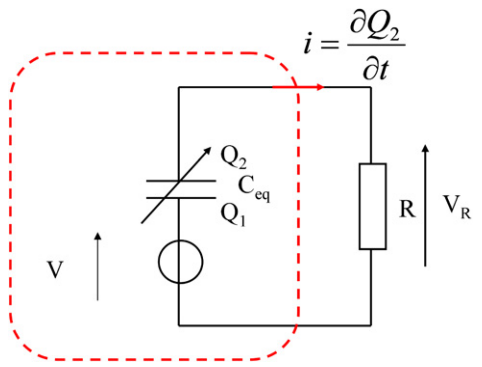

Figure 4. Equivalent electrical model of autonomous dielectric elastomer generator.

3.2. Coupled equations of the soft structure

Let us consider a hyper-elastic law between stress and strain for the dielectric elastomer; the true stresses T_i are written as

$$T_i = \lambda_i \frac{\partial W}{\partial \lambda_i} - p. \tag{5}$$

λ_i is the extension coefficient on the axes (L_1, L_2, L_3), W is the strain energy and p is the hydrostatic pressure. This pressure is unknown and depends on the boundary conditions of the mechanical structure. The strain energy W is classically taken as the Yeoh form (5).

$$W = C_{10}(I_1 - 3) + C_{20}(I_1 - 3)^2 + C_{30}(I_1 - 3)^3. \tag{6}$$

I_1 is the first invariant of the left Cauchy Green deformation tensor (C):

$$I_1 = \lambda_1^2 + \lambda_2^2 + \lambda_3^2. \tag{7}$$

The elastomer (acrylic or silicone for our system) is supposed to work at constant volume (in this case the third invariant of C is $I_3 = \lambda_1\lambda_2\lambda_3 = 1$). The C_{ij} parameters describe the hyper-elastic response and can be calculated by fitting the model to uniaxial tensile test.

Due to the configuration of the generator, the dielectric elastomer supports a pure shear deformation along the L_1 direction. The width (along L_2) is kept constant. A pattern of the scavenger is made of an active part (length L_{1a}) and an inactive part (length L_{1i}). The soft structure is thus described by the mechanical and electrostatic coupled equations, written in (4) and (8) [18].

$$\begin{aligned} mL_{1a0}\frac{\partial^2\lambda}{\partial t^2} = &-\left[2\frac{L_{20}L_{30}}{\lambda}(C_{10} + 2C_{20}(I_1 - 3)\right. \\ &\left. + 3C_{30}(I_1 - 3)^2)\left(\lambda^2 - \frac{1}{\lambda^2}\right)\right] \\ &+ \left[\frac{\partial}{\partial\lambda}\left(\frac{Q_2^2}{2C_{eq}}\right)\right] + F_{ext}. \end{aligned} \tag{8}$$

One can note that the mechanical losses due to the properties of elastomer (viscosity, hysteresis, ...) or brought by the structure (mechanical damping) are not included in this first model. The weight of the structure is neglected here.

Finally, the average output power P_{out}, in steady state, is given by

$$P_{out} = \frac{1}{t_2 - t_1}\int_{t_1}^{t_2} R\left(\frac{\partial Q_2}{\partial t}\right)^2 \partial t \tag{9}$$

where $[t_1 - t_2]$ is the interval of time considered in the steady state.

3.3. Estimation of the equivalent capacitance

To solve the electrostatic equation, the equivalent capacitance of our device must be known. As mentioned above, when a stress is applied to the structure, its dimensions are thus modified and contribute to the variation of the equivalent capacitance according to the imposed stretching. The total equivalent capacitance C_{eq} (λ) can be written as

$$\begin{aligned} C_{eq}(\lambda) &= NC_{eq\_1}(\lambda) \\ C_{eq\_1}(\lambda) &= C_{eq1\_a}(\lambda) + C_{eq1\_i}(\lambda). \end{aligned} \tag{10}$$

C_{eq_1} is the equivalent capacitance of one pattern, N is the number of patterns (for our structure, $N = 3$), C_{eq1_a} stands for the equivalent capacitance of the active part, and C_{eq1_i} is that of the inactive part of one pattern. The equivalent capacitance of the active part is a serial combination of three capacitances, as expressed in (11). We suppose an ideal case without air gap at the end of the stretching phase, as represented in figure 3.

$$\begin{aligned} \frac{1}{C_{eq1\_a}(\lambda)} = &\frac{1}{C_{dielectric1\_a}(\lambda)} \\ &+ \frac{1}{C_{air1\_a}(\lambda)} + \frac{1}{C_{electret1\_a}(\lambda)}. \end{aligned} \tag{11}$$

$C_{dielectric_1\_a}$ is the capacitance of the dielectric elastomer (12), C_{air1_a} stands for the capacitance composed by the air gap, and $C_{electret_1\_a}$ is that developed by the electret (13).

$$C_{dielectric1\_a}(\lambda) = \frac{\varepsilon_0\varepsilon_{rd}L_{1a0}L_{20}}{L_{30}}\lambda^2 \tag{12}$$

$$C_{electret1\_a}(\lambda) = 2\frac{\varepsilon_0\varepsilon_{re}L_{20}l_{electret}}{L_{3e}} \tag{13}$$

with ε_0 the permittivity of free space, ε_{rd} the dielectric constant of the dielectric elastomer and ε_{re} the dielectric constant of the electret. L_{20} stands for the width of the dielectric and electret, L_{30} is the initial thickness of the dielectric elastomer and L_{3e} that of the electret. $l_{electret}$ is the length of the electret.

To estimate the air gap capacitance as a function of the stretch ratio λ, the air gap is cut out into a capacitor of infinitesimal length (dL_1), which can be considered as a plane–plane capacitance (figure 5).

For a given stretching, the infinitesimal capacitance dC_{i_air} is calculated from

$$dC_{i\_air}(\lambda) = \frac{\varepsilon_0 L_{20} dL_1}{L_1 \tan\theta} \tag{14}$$

where $\tan\theta = \dfrac{\sqrt{l_{electret}^2 - \frac{L_{1a0}^2\lambda^2}{4}}}{\frac{L_{1a0}\lambda}{2}}$.

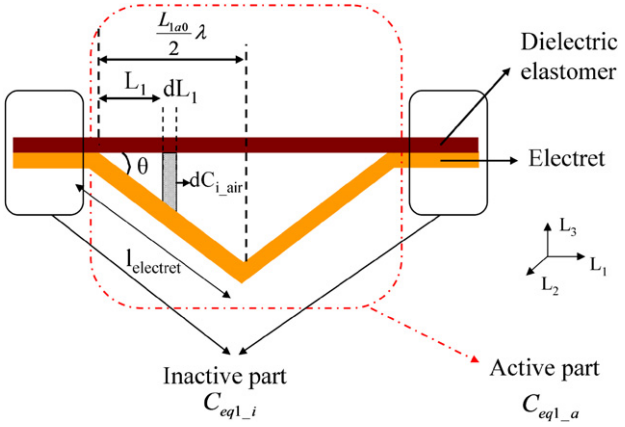

Figure 5. Localization of capacitances on one pattern in a state between the at-rest and the maximal strain positions.

By integrating this expression, the total capacitance of the air gap is

$$C_{\text{air1\_}a}(\lambda) = 2\int_{L_{10}}^{\frac{L_{1a0}\lambda}{2}} \mathrm{d}C_{i\_\text{air}}(\lambda)$$

$$= \left[\frac{2\varepsilon_0 L_{20} L_{1a0}\lambda}{\sqrt{4l_{\text{electret}}^2 - L_{1a0}^2\lambda^2}} \ln x\right]_{L_{10}}^{\frac{L_{1a0}\lambda}{2}}. \quad (15)$$

L_{10} stands for the length of the first infinitesimal capacitance. This value must be small enough to allow a good precision. We arbitrarily choose an L_{10} of 1 μm.

Let us now consider the equivalent capacitance of inactive parts; this equivalent capacitance is also a serial combination of electret and dielectric elastomer. Note that these inactive parts do not suffer any deformation, thus the equivalent capacitance is independent of stretching and can be written as

$$\frac{1}{C_{\text{eq1\_}i}} = \frac{1}{C_{\text{dielectric1\_}i}} + \frac{1}{C_{\text{electret1\_}i}} \quad (16)$$

where $C_{\text{dielectric1\_}i} = \frac{\varepsilon_0\varepsilon_{\text{rd}} L_{1i} L_{20}}{L_{30}}$ and $C_{\text{electret1\_}i} = 2\frac{\varepsilon_0\varepsilon_{\text{re}} L_{1i} L_{20}}{L_{3e}}$.

Finally, the equivalent capacitance of one pattern, calculated by (10), is compared to an FEM simulation (electrostatic module—COMSOL). This simulation takes into account all edge effects and computes a true equivalent capacitance of our structure thanks to the sample's geometry and the electrical energy density value. The equivalent capacitance of one pattern, with the geometric parameters presented in figure 3, is reported in figure 6.

Figure 6(a) shows the electrical field given by FEM software—COMSOL Multiphysics. The potential of the upper electrode was fixed to a value and the lower electrode was set to the ground. The boundary condition between the electret and air gap is set to continuity. The energy density computed by COMSOL can be used to calculate the equivalent capacitance of our structure. The results, shown in figure 6(b), illustrate that the analytical model from (10)–(13), (15) and (16) fitted well to the values computed by COMSOL. The small difference observed (inset of figure 6(b)) can be explained by all geometric and edge effects which were considered by COMSOL. However, the majority of the values, especially extreme capacitances (maximum and minimum), are similar with the two approaches, making it possible to estimate with a good precision the output power. Thus, the analytic calculation of the equivalent capacitance will be used to simulate the overall behavior of the structure and to estimate the output power. Thanks to the analytical model implemented in Matlab/Simulink, the system can be optimized according to its geometric and electrical parameters.

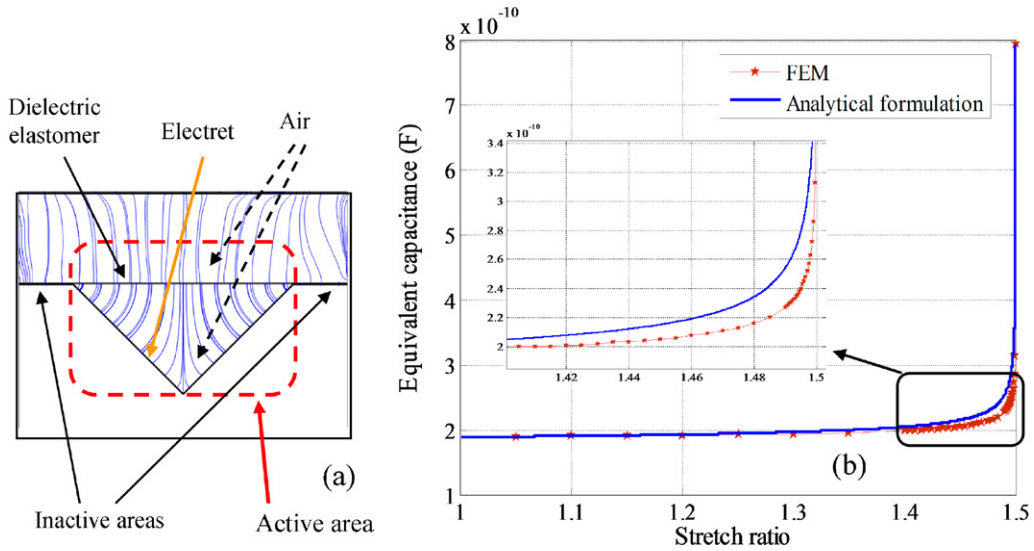

Figure 6. (a) Distributed electrical field in one pattern and (b) capacitance of one active part of the device versus stretch ratio.

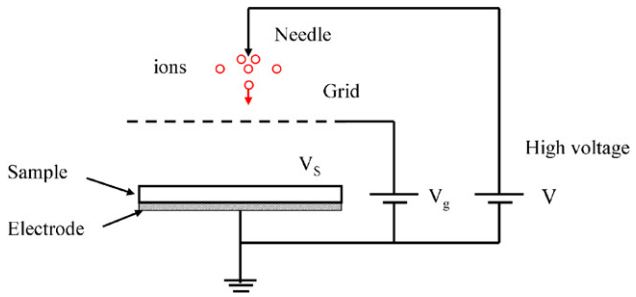

Figure 7. Corona discharge equipment used to create electrets.

4. Experimental setup and results

4.1. Materials

The dielectric elastomer used is silicone PDMS provided by Danfoss PolyPower (Wacker RT 625), which has a thickness of 40 μm. From a mechanical point of view, the elastomer develops a hyper-elastic behavior which can be expressed by the Yeoh strain energy function, with $C_{10} = 64.2$ kPa, $C_{20} = 147.63$ kPa and $C_{30} = -184.56$ kPa [19]. Carbon conductive grease from MG Chemicals is used to make compliant electrodes following the material deformation. The main electrical parameter of this structure (dielectric elastomer and electrodes) is its permittivity. Related to our previous study, this permittivity is approximately $\varepsilon_{rd} = 3.1$ at room temperature. However, this value is not constant; it decreases as a function of strain ($\varepsilon_{rd} = 2.6$ at 50% strain—pure-shear deformation mode) [20]. A simple (linear) relation between the permittivity of the dielectric elastomer and the strain has been introduced into our model for a better accuracy.

Thin layer electrets with a low dielectric permittivity (low k) such as CYTOP, parylene, and Teflon can develop a high surface potential [21–23]. Several works have been focused on the stability of these polymers with studies of the surface potential decay as a function of several parameters such as temperature, relative humidity, fabrication process, initial potential, and size of the electret [24, 25]. From this state of art, Teflon FEP from DuPont was selected because of its low cost and charge stability. This polymer is a commercial sheet available in different thicknesses (25 μm or 50 μm) and able to keep a high theoretical surface potential for more than 10 years. A positive or negative corona discharge is used to charge the Teflon polymer (figure 7). It consists of a needle–grid–plate structure whose needle is subjected to a strong electrical field smaller than the value of breakdown, but high enough to create plasma. These ions are accelerated and projected onto the surface of the sample. This mechanism results in the implantation of charges at the surface or into the volume of the material. A grid, located between the needle and the sample, can be used to control and fix the surface potential of the electret. In this configuration, at the end of the corona discharge, the initial surface potential V_s of the sample is equal to the grid potential V_g.

Nonetheless, dielectrics are not perfect insulators and implanted charges can move both on the surface and inside the material or can be compensated by other charges or environmental conditions, leading to disappearance of these charges. In order to select the more stable electrets for our application, we carried out several experiments focused on surface decay of Teflon FEP under various positive/negative potentials for two thicknesses of material. The results are reported in figure 8.

In this work, a needle voltage of ±5 kV was applied for 3 min. After charging, the samples were stored in a small plastic box at room temperature and ambient relative humidity. The surface potential as a function of time was measured regularly thanks to a contactless electrostatic voltage probe (TREK® 347 electrostatic voltmeter). As seen in figure 8, the negatively charged FEP films develop excellent charge stability even after 196 days. Moreover, we can note that the initial value of the surface potential, measured just after the negative corona discharge, is similar to the voltage grid, confirming the absence of a fast flow of some charges. On the other hand, the positive surface potential decay is evident, and all the more when the initial potential is high. These different trends can be interpreted by the distribution of charges on the surface or into the polymer film: the positive

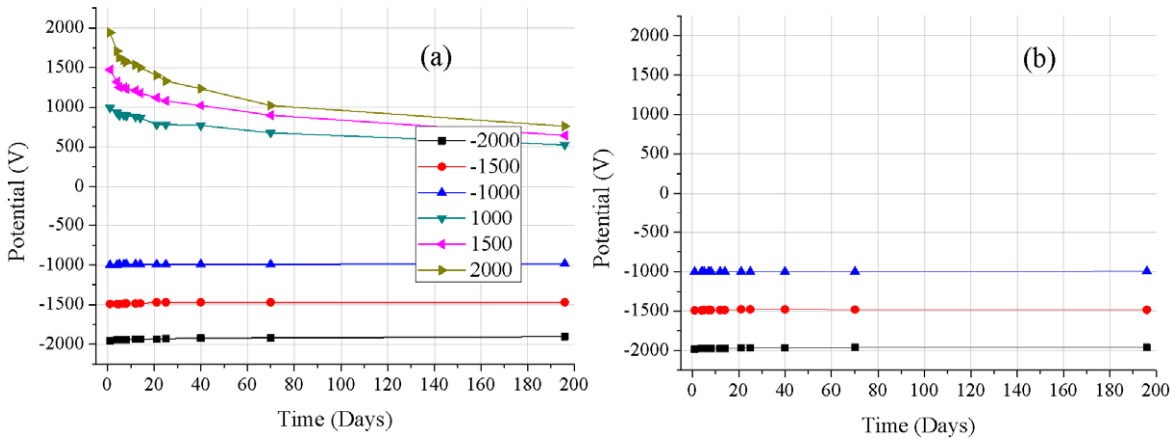

Figure 8. Surface potential decay for Teflon FEP (a) 25 μm thickness and (b) 50 μm thickness.

Table 1. Summary of some parameters of our electret–dielectric elastomer generator.

Parameter		Symbols	Material	
			Danfoss PolyPower	Teflon FEP
Initial thickness (μm)			40	50
Maximum stretch (λ_{L_1}, 1)		λ_m	(1.5, 1)	(1, 1)
Relative dielectric constant	Without stretch	ε_r	3.1	2.1
	At maximum stretch		2.6	—
Yeoh model (kPa)		C_{10}	64.2	
		C_{20}	147.63	—
		C_{30}	−184.56	
Prototype				
Electret potential (V)		V	−1000	
Each pattern	Length of active part (cm)	L_{1a}	2	
	Length of inactive part (cm)	L_{1i}	0.5	
	Width (cm)	L_{20}	2.5	
	Maximum stretch (–)	λ_m	1.5	
Number of patterns (–)		N	3	
Excitation frequency (Hz)		f	1	

charges are located especially at the surface and disappear more easily, while the negative ones are present in both the surface and the volume of the material, allowing a better stability [26]. These results underline that the negatively charged Teflon FEP is an excellent electret: the surface potential of this electret charged at −1000 V decreases by only 1 V after 70 days and by 6 V after 196 days. In addition, as clearly shown in figure 8, the thickness of Teflon FEP does not have any influence on the value of the stored charge and its flow. Consequently, Teflon FEP 50 μm thick (easier to handle than 25 μm) and charged up to −1000 V was selected to build our new scavenger.

4.2. Prototype and experimental setup

To demonstrate this new concept of dielectric elastomer generator, we developed a prototype to scavenge mechanical energy for example during human motion and especially on a knee joint. Because of the available space behind the knee, the total area of the structure is chosen to be 9 cm by 2.5 cm. Depending on geometrical considerations, a maximal deformation of 50% at 1 Hz is achievable with an adequate use of active and inactive area, focusing the deformation on the active part [8]. Moreover, a larger active area, namely a wider electret, insures a more important scavenged energy [18]. To satisfy geometric and practical specifications (size, active deformation, hand made, ...), the structure is therefore made of three patterns with an active length of 2 cm and a passive length of 1 cm (0.5 cm each side). The serpentine frame insures a maximal deformation of 50% in the active area. In table 1, the main parameters of our prototype are summarized.

The structure presented in figure 3 was hand made and mounted on a test setup. The structure was mechanically clamped on one side and can move at a frequency of 1 Hz in the L_1 direction thanks to a mechanical system, i.e. a slider–crank and an electrical motor. The area strain of the dielectric elastomer was calculated from a video post-treatment. Detailed attention was paid to the air gap and especially its final value. To determine the harvested power, the device was connected to an electrical load R, and the output voltage was monitored by an electrostatic voltage probe (Monroe ISOPROBE® Electrostatic Voltmeter 244). Figure 9 shows the dielectric elastomer generator and the test setup.

4.3. Results

Figure 10 reports the output electrical measurement (theory and experiment) on a resistive load of 99 MΩ for the manufactured structure solicited at 1 Hz.

The mechanical excitation and the electrical output voltage have the same frequency, namely 1 Hz. One notes that the structure produces a high output voltage (peak to peak voltage of several hundreds of volts), characteristic of electrostatic generators. The output voltage develops the typical trend of rigid electret generators [14, 23, 27], illustrating that mechanical energy was successfully scavenged by our device. One observes (figure 10(a)) that experimental and theoretical curves do not fit very well: the same shape but different extreme values. These differences are due to the residual air gap remaining in the maximum stretched state. Ideally, the maximum energy is obtained when a maximum capacitance variation is reached. It would be specifically obtained if no air gap existed between the dielectric layer and the electret layer at maximum strain state. However, in practical applications, a thin layer of air always remains because of a non-perfect contact. Thereby, the experimental value of maximum capacitance is much smaller than that of the ideal theoretical case. The harvested energy is consequently much smaller than expected. We deduced from our measurements an air gap of about 500 μm at maximum stretching. This air gap value was embedded into our analytical model, named 'adjusted theoretical', and the corresponding output voltage is plotted in figure 10(b). One can note that the experiments are close to this corrected

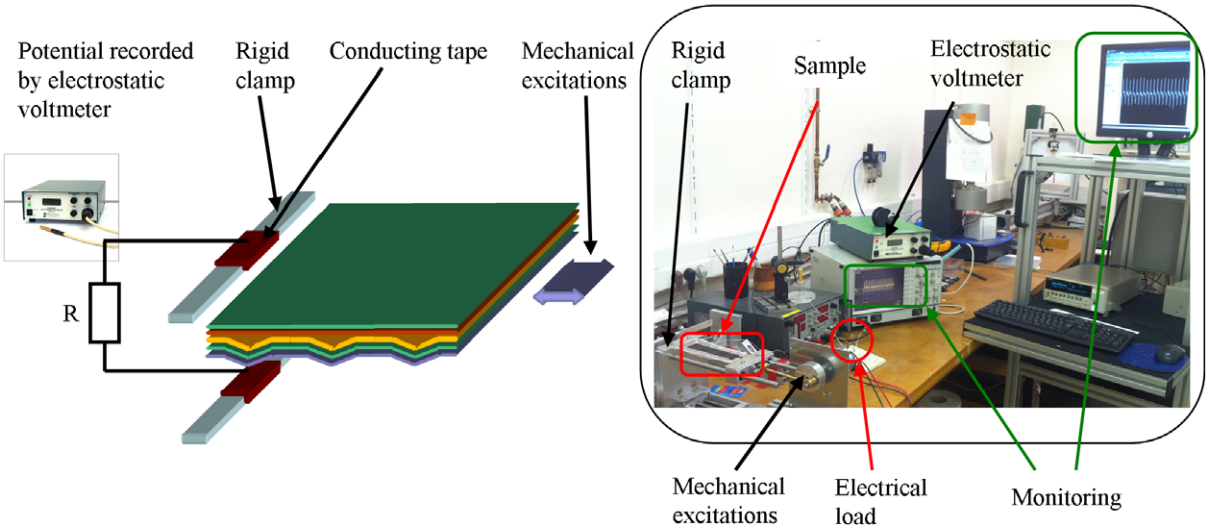

Figure 9. Dielectric elastomer generator and experimental setup.

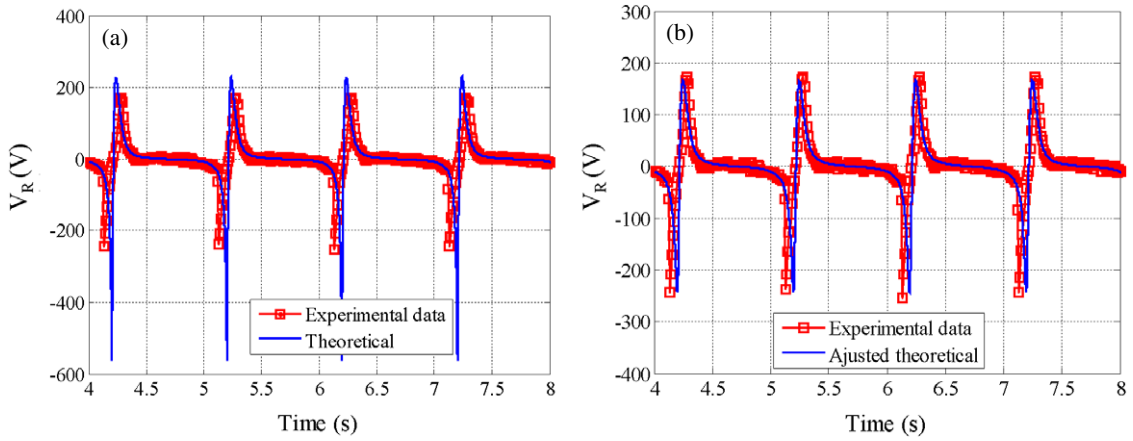

Figure 10. Experimental output voltage for $R = 99$ MΩ. (a) Experimental data and ideal theoretical model and (b) experimental data and adjusted theoretical model.

model for both positive and negative extreme values. The light variation observed in the shape of the curves during the switch phase from minimal to maximal values is explained by the uncertainty of our calculation predicting the value of the equivalent capacitance as presented in figure 6(b). With regard to the oscillations on the experimental results (figure 10), they can be assigned to the different losses (dielectric and mechanical), not taken into account in the model, but also to the measurement inaccuracy (sensitivity of the test setup).

In order to better validate our model, we measured the capacitance of the structure for various stretchings from an HP4284A *LCR* meter. As observed in figure 11(a), the capacitance is overestimated by the model. As the structure is hand made, desired dimensions cannot be respected perfectly. An error of a few per cent (especially of the air gap, as already discussed) will be able to induce a reduction in the value of the capacitance, thus leading to a drop of the output voltage. However, the relative error between measurements and predicted values of this equivalent capacitance (about 8%) can be considered weak regarding the output power obtained (figure 11(b)), and thus our model can be used for further optimizations. As our device is an electrostatic generator, the maximum output power is obtained for a matched load. Output power on various loads was thus recorded for the structure. This average power is compared to the adjusted theoretical case with a residual air gap of 500 μm (figure 11(b)).

To summarize, our adjusted theoretical model constitutes a good representation of the output power really available with our prototype. Our structure makes it possible to scavenge 33 μW on a resistance load of 99 MΩ. In an ideal case, a power of 85 μW is expected (figure 11(b)). As the density of the polymer is about 1 g cm^{-3} and from the volume of our structure, the density of produced energy is 0.55 mJ g^{-1}.

To supplement the tests on the capabilities of our autonomous elastomer generator, we use it now in a realistic chain for energy harvesting. For this, the alternative output voltage of the dielectric generator is rectified from a rectifier constituted of four diodes (1N3595—Fairchild Semiconductor) and a storage capacitor (1.2 nF) is connected at the end of this rectifier (figure 12(a)). This storage capacitor was precisely characterized through its measurement starting from an impedance meter (Novocontrol BDS 20) at the frequency of 1 Hz. A capacitance $C_p = 1.27$ nF is obtained

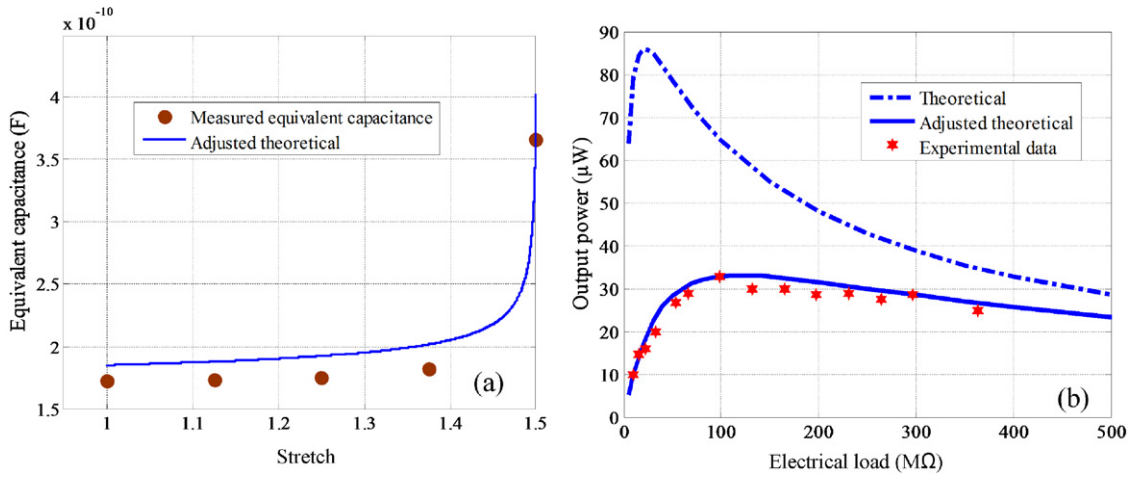

Figure 11. (a) Comparison between the measured capacitance and the model. (b) Output power versus the external load.

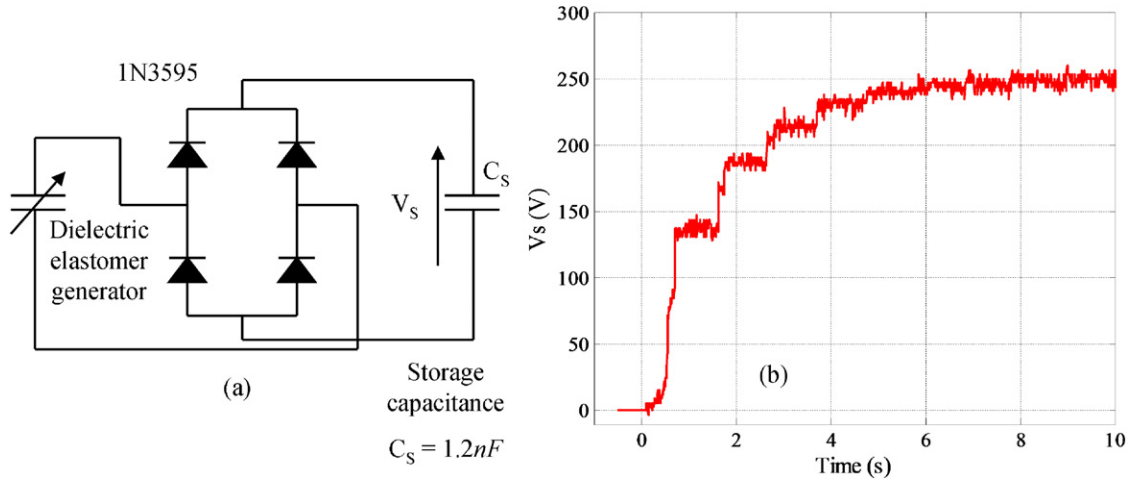

Figure 12. (a) Power management chain and (b) charge in the storage capacitor (1.2 nF). Input mechanical excitation was set at 1 Hz and strain at 50%.

and the resistance associated with this capacitance is $R_p = 4.8$ GΩ. In figure 12(b), the voltage across the storage capacitor is boosted from 0 to 250 V after 5 s, namely five cycles. Consequently, the scavenged energy stored in the capacitor is estimated at around 39.7 μJ, which covers energy of 7.95 μJ per cycle (corresponding to an output power of 7.95 μW because the cycle is 1 Hz). The specific energy density of our device is approximately 0.008 mJ g^{-1}.

In order to estimate the efficiency of power management, we applied our model with the case of the true capacitance used for experiments. In this configuration, the electrical resistance load R in figure 4 must be replaced by a parallel (R_p, C_p) component with $R_p = 4.8$ GΩ, $C_p = 1.27$ nF, and (4) becomes

$$i(t) = \frac{\partial Q_2}{\partial t} = \frac{1}{1 + \frac{C_p}{C_{eq}}} \times \left[\frac{V}{R_p} - Q_2 \left(\frac{1}{R_p C_{eq}} - \frac{C_p}{C_{eq}^2} \frac{\partial C_{eq}}{\partial t} \right) \right]. \quad (17)$$

A calculated output power of 19.6 μW per cycle (1 Hz) is obtained. Compared to the measured output power of 7.95 μW incorporating the rectifier, efficiency from only 42% is obtained. This low efficiency is due to leakage losses in the rectifiers.

4.4. Improvement of our prototype: impact of operating frequency and electret potential

To summarize our results, for a cycle at 1 Hz, the average output power is theoretically about 85 μW on an optimal load of 20 MΩ and experimentally about 33 μW on a load of 99 MΩ (figure 11(b)). The density of the energy produced is experimentally 0.55 mJ g^{-1} and can grow to 1.42 mJ g^{-1}, corresponding to the ideal case. It should be noted that flexible structures using piezoelectric and electrostrictive polymers have been developed to scavenge energy. For example, Shenck *et al* reported a power of 1.3 mW on the structure of 65 cm^2 based on PDVF polymer (16 layers of 28 μm thickness for each one) embedded into shoes, on an electrical resistance of 250 kΩ at 0.9 Hz [28]; this leads to an energy density of

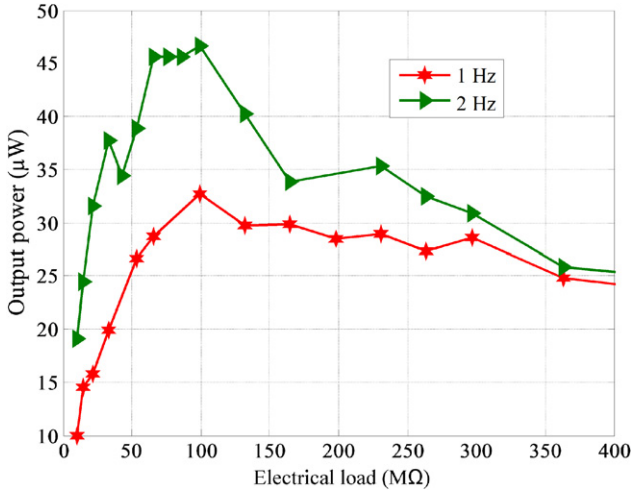

Figure 13. Harvested power versus electrical load for various frequencies. Input mechanical excitation was set at 1 Hz or 2 Hz and strain at 50%.

0.27 mJ g^{-1} (assuming that the specific mass of PVDF is 1.78 g cm^{-3}). With regard to electrostrictive polymers, Lallart *et al* [29] showed an energy density of about 0.056 mJ g^{-1} scavenged by their device (5 cm^2 and 50 μm thickness) made by P(VDF–TrFE–CFE)–1% C under 10 MV μm^{-1} and 0.5% strain at 100 Hz. More recently, by studying an electrostrictive transducer at low frequency, Meddad *et al* [30] noted a power of 0.3 μW converted using PU–1 wt% C (6.4 cm^2 and 52 μm thickness) under 10 V μm^{-1} with 0.5% strain at 3 Hz. This represents an energy density of 0.0082 mJ g^{-1} (the specific mass of PU–1 wt% C is 1.1 g cm^{-3}). Finally, one can underline that the experimental energy density obtained by our device using dielectric elastomer and electret is at least twice as significant as that reached by piezoelectric polymer and ten times that obtained with electrostrictive polymer.

The high theoretical energy density obtained in our case allows us to project interesting potentialities for our structure. For this, the serpentine shape must be optimized (by industrializing the manufacturing process for example) in order to reduce the residual air gap. Before this, one can be interested in the influence of the frequency but also in the value of the surface potential of electret on the output power obtained.

The increase in the operating frequency will induce not necessarily an increase in the energy density but surely a boost in output power. For example, human motion can vary from 1 Hz (walk) to 2 Hz (run) and the experimental harvested power of our prototype at these frequencies is shown in figure 13.

As expected, for a given electrical load, the output power is much greater with higher frequency. This tendency is respected strictly on a wide range of resistance loads with, always, a maximum of output power with a load of 99 MΩ. At this optimum load, 46.6 μW (at 2 Hz) is reached. This value makes it possible to obtain an energy density of 0.39 mJ g^{-1} for one cycle. One can note that, although energy density decreases as frequency increases, more output power is produced when the structure works at high frequencies.

Another way to enhance the output power of the structure is the increase of the surface potential of the electret. To investigate this capability, we choose to apply our 'adjusted theoretical' model, validated previously with a surface potential of −1000 V (figure 11(b)). Output power obtained with surface potentials of −1500 V or −2000 V is reported in figure 14 and demonstrates without ambiguity the interest of such electret–dielectric elastomer generators. This output power can be expressed as a function of the square of the surface potential, as demonstrated by Boland *et al* [13]. We reported this behavior in figure 14(b) for always the same load of 99 MΩ because this value remains practically optimal for all the surface potentials. Output power of 150 μW (equivalent to 4.16 mJ g^{-1}) is achievable with an electret potential of −2000 V. The potential of −2000 V for a Teflon FEP electret is credible, as confirmed in figure 8.

To finish, let us now compare the energy density of our generator to a classic DEG (with external bias voltage) [8] and to a centimetric rigid electret generator [14]. It should be

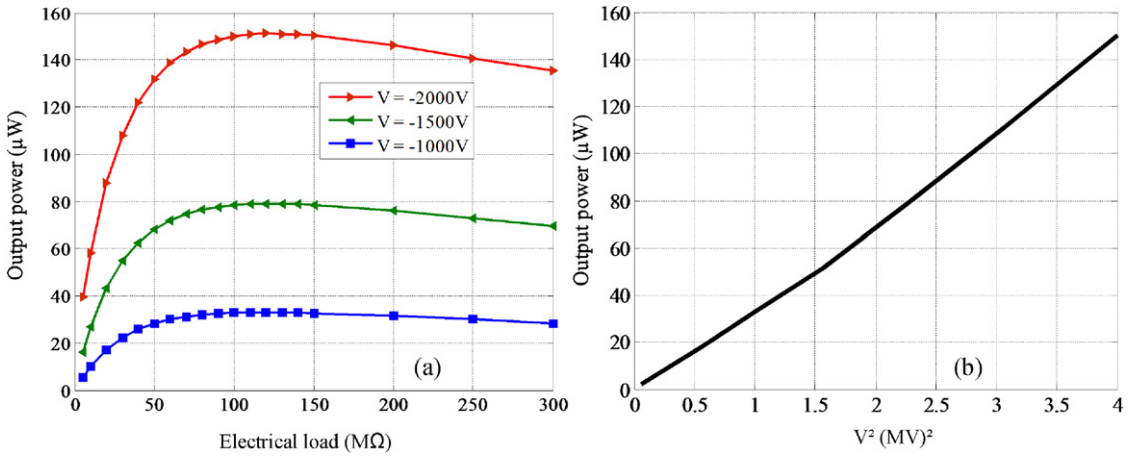

Figure 14. Predicted output power. (a) Output power versus electrical load for various values of electret potential. (b) Output power versus V^2.

Table 2. Main characteristics of three generators.

		This work		Classic DEG [8]		Electret generator [14]
Active surface	cm^2	15		15		9
Frequency	Hz	1	2	1		2
Bias voltage or electret potential	V	−1000	−1000	170	1000	—
Maximal output voltage (load) (peak–peak)	V	400		340	2000	—
Average output power (measured)	μW	33	46.6	100		40
Energy density (measured)	mJ g^{-1}	0.55	0.38	2.1		—
Energy density (expected)	mJ g^{-1}	1.42	—		37	—
Power management		Diode rectifier (low cost/low size)		External high voltage supply + diode		Diode rectifier (low cost/low size)

noted that the maximum output power of an electret generator and our electret–dielectric elastomer generator is matched for an optimal value of electrical resistance (99 MΩ for our generator). Hence, we report the maximum output power and the energy density for an optimal load, compared to the classic DEG in the table 2. The power management associated is also presented but the efficiency is not considered here.

The two first structures have the same area (15 cm^2). All the generators work at low frequency: 1 Hz for both using dielectric elastomer and 2 Hz for our new dielectric elastomer generator and the classic electret generator (table 2). Up to now, at 1 Hz, our new structure scavenges less than the classic DEG: 33 μW instead of 100 μW because of the texture (serpentine) imposed by the non-deformable electret. However, 83 μW is expected with this hybrid structure, namely an energy density of 1.42 mJ g^{-1}, which is close to the energy density obtained with the classic DEG structure (2.1 mJ g^{-1}). By optimizing the serpentine frame and the potential of the electret, 100 μW can be easily achieved for the same size of structure. Finally, compared to a classic electret generator [14], our structure develops comparable performances: scavenging of the same level of energy under low frequency. Moreover, as our scavenger uses only four diodes and no external voltage supply, it could be implemented in wearable application whereas the classic DEG structure cannot.

5. Conclusion

A new concept of electrostatic generator was initially proposed, then modeled and finally manufactured and tested. This structure combines a dielectric elastomer (silicone PolyPower^{TM}) and an electret (Teflon^{TM}) in order to build an autonomous soft generator requiring no external bias voltage or complex power circuit to scavenge mechanical energy. Our transducer is compliant, lightweight, low cost and reaches 0.55 mJ g^{-1} with an electret potential of −1000 V for an active strain of 50%. Moreover, the power management is quite simple, which makes it possible to implement this electrostatic generator in wearable or portable applications such as e-textile applications. Once optimized in its design, such a soft generator could produce energy density up to 1.42 mJ g^{-1} with electret potential of −1000 V. An energy density of 4.16 mJ g^{-1} is expected with an electret potential of −2000 V.

References

[1] Pozzi M, Aung M S H, Zhu M, Jones R K and Goulermas J Y 2012 The pizzicato knee-joint energy harvester: characterization with biomechanical data and the effect of backpack load *Smart Mater. Struct.* **21** 075023

[2] Paradiso J A and Starner T 2005 Energy scavenging for mobile and wireless electronics *IEEE Pervasive Comput.* **4** 18–27

[3] Koh S J, Keplinger C, Li T F, Bauer S and Suo Z G 2011 Dielectric elastomer generators: how much energy can be converted? *IEEE/ASME* **16** 33–41

[4] Chiba S, Waki M, Kornbluh R and Pelrine R 2008 Innovative power generators for energy harvesting using electroactive polymer artificial muscles *Proc. SPIE* **6927** 692715

[5] Kornbluh R D, Pelrine R, Prahlad H, Wong-Foy A, Mccoy B, Kim S, Eckerle J and Low T 2011 From boots to buoys: promises and challenges of dielectric elastomer energy harvesting *Proc. SPIE* **7976** 797605

[6] Iskandarani Y H, Jones R W and Villumsen E 2009 Modeling and experimental verification of a dielectric polymer energy scavenging cycle *Proc. SPIE* **7287** 728768

[7] McKay T, O'Brien B, Calius E and Anderson I 2010 An integrated dielectric elastomer generator model *Proc. SPIE* **7642** 764216

[8] Jean-Mistral C, Basrour S and Chaillout J-J 2008 Dielectric polymer: scavenging energy from human motion *Proc. SPIE* **6927** 692716

[9] Eitzen L, Graf C and Maas J 2011 Cascaded bidirectional flyback converter driving DEAP transducers *Proc. IECON* pp 1226–31

[10] Keplinger C, Kaltenbrunner M, Arnold N and Bauer S 2010 Röntgen's electrode-free elastomer actuators without electromechanical pull-in instability *Proc. Natl Acad. Sci. USA* **107** 4505–10

[11] Jean-Mistral C, Vu-Cong T and Sylvestre A 2012 Advances for dielectric elastomers generators: replacement of high voltage supply by electret *Appl. Phys. Lett.* **101** 162901

[12] Despesse G, Chaillout J J, Jager T, Léger J M, Vassilev A, Basrour S and Charlot B 2005 High damping electrostatic system for vibration energy scavenging *Proc. sOc-EUSAI'05* pp 283–6
[13] Boland J S, Chao Y H, Suzuki Y and Tai Y C 2003 Micro electret power generators *Proc. MEMS'03* pp 538–41
[14] Naruse Y, Matsubara N, Mabuchi K, Izumi M and Suzuki S 2009 Electrostatic micro power generation from low-frequency vibration such as human motion *J. Micromech. Microeng.* **19** 094002
[15] Shimizu N and Electronics Nikkei 2008 Omron prototypes compact, simple vibration powered generator *Nikkei Electronics* http://techon.nikkeibp.co.jp/english/NEWS_EN/20081117/161303
[16] Edamoto M, Suzuki Y, Kasagi N, Kashiwaki K, Morizawa Y, Yokoyama T, Seki T and Oba M 2009 Low-resonant-frequency micro electret generator for energy harvesting application *Proc. MEMS'09* pp 1059–62
[17] Boisseau S, Despesse G and Sylvestre A 2010 Optimization of an electret-based energy harvester *Smart Mater. Struct.* **19** 075015
[18] Jean-Mistral C, Vu Cong T and Sylvestre A 2012 Flexible autonomous scavengers: the combination of dielectric polymers and electrets *Proc. SPIE* **8340** 834029
[19] Czech B, Van Kessel R, Bauer P, Ferreira J A and Wattez A 2010 Energy harvesting using dielectric elastomers *Proc. EPE-PEMC'2010* pp S4-18–23
[20] Vu-Cong T, Jean-Mistral C and Sylvestre A 2012 Impact of the nature of the compliant electrodes on the dielectric constant of acrylic and silicone electroactive polymers *Smart Mater. Struct.* **21** 105036
[21] Lo H and Tai Y-C 2008 Parylene-based electret power generators *J. Micromech. Microeng.* **18** 104006
[22] Kotrappa P 2008 Long term stability of electrets used in electret ion chambers *J. Electrost.* **66** 407
[23] Sakane Y, Suzuki Y and Kasagi N 2008 The development of a high-performance perfluorinated polymer electret and its application to micro power generation *J. Micromech. Microeng.* **18** 104011
[24] Sessler G M 1998 *Electrets* 3rd edn
[25] Erhard D P, Lovera D, Von Salis-Soglio C, Giesa R, Altstädt V and Schmidt H-W 2010 Recent advances in the improvement of polymer electret films *Adv. Polym. Sci.* **228** 155–207
[26] Giacometti J A, Fedosov S and Costa M M 1999 Corona charging of polymers: recent advances on constant current charging *Braz. J. Phys.* **29** 269–79
[27] Boisseau S, Despesse G, Ricart T, Defay E and Sylvestre A 2011 Cantilever-based electret energy harvesters *Smart Mater. Struct.* **20** 105013
[28] Shenck N S and Paradiso J A 2001 Energy scavenging with shoe-mounted piezoelectrics *IEEE Micro* **21** 30–42
[29] Lallart M, Cottinet P-J, Lebrun L, Guiffard B and Guyomar D 2010 Evaluation of energy harvesting performance of electrostrictive polymer and carbon-filled terpolymer composites *J. Appl. Phys.* **108** 034901
[30] Meddad M, Eddiai A, Guyomar D, Belkhiat S, Cherif A, Yuse K and Hajjaji A 2012 An adaptive prototype design to maximize power harvesting using electrostrictive polymers *J. Appl. Phys.* **112** 054109